THE JOURNAL OF BIOLOGICAL CHEMISTRY VOL. 289, NO. 38, pp. 26584–26596, September 19, 2014

Overexpression of *Galnt3* in Chondrocytes Resulted in Dwarfism Due to the Increase of Mucin-type *O*-Glycans and Reduction of Glycosaminoglycans*

Received for publication, February 7, 2014, and in revised form, August 4, 2014 Published, JBC Papers in Press, August 8, 2014, DOI 10.1074/jbc.M114.555987

Carolina Andrea Yoshida[‡1], Tetsuya Kawane[‡1], Takeshi Moriishi[‡1], Anurag Purushothaman[§1,2], Toshihiro Miyazaki[‡], Hisato Komori[‡], Masako Mori[‡], Xin Qin[‡], Ayako Hashimoto[‡¶], Kazuyuki Sugahara[§‖], Kei Yamana[**], Kenji Takada[¶], and Toshihisa Komori[‡3]

*From the [‡]Department of Cell Biology, Unit of Basic Medical Sciences, Nagasaki University Graduate School of Biomedical Sciences, 1-7-1 Sakamoto, Nagasaki 852-8588, Japan, the [§]Department of Biochemistry, Kobe Pharmaceutical University, Kobe 658-0003, Japan, the [¶]Department of Orthodontics and Dentofacial Orthopedics, Graduate School of Dentistry, Osaka University, Suita, Osaka 565-0871, Japan, the [‖]Proteoglycan Signaling and Therapeutics Research Group, Faculty of Advanced Life Science, Hokkaido University Graduate School of Life Science, Frontier Research Center for Post-Genomic Science and Technology, Sapporo 001-0021, Japan, and the **Teijin Institute for Biomedical Research, Teijin Ltd., Hino, Tokyo 191-8512, Japan*

Background: The physiological roles of mucin-type *O*-glycosylation in proteoglycans are completely unknown.
Results: Overexpression of *Galnt3* (UDP-*N*-acetyl-α-D-galactosamine:polypeptide *N*-acetylgalactosaminyltransferase 3) in chondrocytes reduced aggrecan and caused dwarfism.
Conclusion: *N*-acetylgalactosamine (GalNAc)-transferases increase mucin type *O*-glycans but reduce glycosaminoglycans leading to the reduction of aggrecan probably through competition with xylosyltransferases.
Significance: GalNAc-transferases regulate chondrocyte proliferation and maturation by modifying the glycosylation of aggrecan.

Galnt3, UDP-*N*-acetyl-α-D-galactosamine:polypeptide *N*-acetylgalactosaminyltransferase 3, transfers *N*-acetyl-D-galactosamine to serine and threonine residues, initiating mucin type *O*-glycosylation of proteins. We searched the target genes of Runx2, which is an essential transcription factor for chondrocyte maturation, in chondrocytes and found that *Galnt3* expression was up-regulated by Runx2 and severely reduced in *Runx2*$^{-/-}$ cartilaginous skeletons. To investigate the function of Galnt3 in chondrocytes, we generated *Galnt3*$^{-/-}$ mice and chondrocyte-specific *Galnt3* transgenic mice under the control of the *Col2a1* promoter-enhancer. *Galnt3*$^{-/-}$ mice showed a delay in endochondral ossification and shortened limbs at embryonic day 16.5, suggesting that Galnt3 is involved in chondrocyte maturation. *Galnt3* transgenic mice presented dwarfism, the chondrocyte maturation was retarded, the cell cycle in chondrocytes was accelerated, premature chondrocyte apoptosis occurred, and the growth plates were disorganized. The binding of *Vicia villosa* agglutinin, which recognizes the Tn antigen (GalNAc-*O*-Ser/Thr), was drastically increased in chondrocytes, and aggrecan (Acan) was highly enriched with Tn antigen. However, safranin O staining, which recognizes glycosaminoglycans (GAGs), and Acan were severely reduced. Chondroitin sulfate was reduced in amount, but the elongation of chondroitin sulfate chains had not been severely disturbed in the isolated GAGs. These findings indicate that overexpression of *Galnt3* in chondrocytes caused dwarfism due to the increase of mucin-type *O*-glycans and the reduction of GAGs, probably through competition with xylosyltransferases, which initiate GAG chains by attaching *O*-linked xylose to serine residues, suggesting a negative effect of Galnt family proteins on Acan deposition in addition to the positive effect of Galnt3 on chondrocyte maturation.

In the cartilage anlage, chondrocytes lay an exclusive extracellular matrix and proceed to sequential phases of proliferation, prehypertrophy, and hypertrophy. Hypertrophic cells then mineralize the extracellular matrix surrounding them and die through apoptosis (1, 2). This differentiation process results in the formation of a cartilaginous growth plate responsible for elongation of the bone. Finally, blood vessels, together with osteoblast and osteoclast progenitors, invade the anlage through the mineralized hypertrophic region, degrade the cartilage, and replace it with bone.

The extracellular matrix produced by growth plate chondrocytes is rich in collagens and proteoglycans (3). Proteoglycans are made of a core protein to which disaccharide chains called sulfated glycosaminoglycans (GAGs)[4] composed of repeating disaccharide units, including chondroitin sulfate, dermatan sulfate, keratan sulfate, and heparan sulfate, are covalently bound (4). The acidic GAGs have the capacity to hold water, which makes the cartilage resilient (5). Moreover, proteoglycans in cartilage regulate the diffusion of growth factors and bind different functional proteins like fibroblast growth factors and hedgehog proteins, regulating cell signaling pathways

* This work was supported by a grant from the Ministry of Education, Culture, Sports, Science, and Technology, Japan, and the President's Discretionary Fund of Nagasaki University.
[1] These authors contributed equally to this work.
[2] Present address: Dept. of Pathology, University of Alabama at Birmingham, Birmingham, AL 35294.
[3] To whom correspondence should be addressed. Tel.: 81-95-819-7630; Fax: 81-95-819-7633; E-mail: komorit@nagasaki-u.ac.jp.

[4] The abbreviations used are: GAG, glycosaminoglycan; Acan, aggrecan; VVA, *V. villosa* agglutinin; PAS, periodic acid-Schiff; E*n*, embryonic day *n*.

(6–8). The importance of the cartilage extracellular matrix can be noted in the phenotypes of humans or mice carrying mutations in genes encoding extracellular matrix proteins (9, 10).

Mucin-type *O*-glycosylation, consisting of glycans attached via *O*-linked *N*-acetyl-D-galactosamine (GalNAc) to serine and threonine residues, is one of the most abundant forms of protein glycosylation in animals, and it is controlled by a large family of up to 20 homologous Galnt genes encoding UDP-GalNAc:polypeptide GalNAc-transferases (11). It is well known that Galnt3 regulates phosphate homeostasis through glycosylation of FGF23. Loss-of-function mutations in the *GALNT3* gene result in underglycosylation and consequent protein degradation of FGF23, leading to hyperostosis-hyperphosphatemia syndrome or tumoral calcinosis (12–16).

We searched the target genes of Runx2, which is essential for chondrocyte maturation (17, 18), in chondrocytes, and found that *Galnt3* expression is induced by Runx2 and is severely reduced in the cartilaginous tissues of *Runx2*$^{-/-}$ mice. To investigate the function of Galnt3 in chondrocytes, we generated *Galnt3*$^{-/-}$ mice and chondrocyte-specific *Galnt3* transgenic mice. Although many Galnt family genes were expressed in cartilaginous tissues during embryogenesis, the process of endochondral ossification was retarded in *Galnt3*$^{-/-}$ mice at the embryonic stage. *Galnt3* transgenic mice showed severely shortened endochondral bones, and the cartilage extracellular matrix contained very low amounts of aggrecan (Acan) proteoglycan. Increase of mucin-type *O*-glycosylation by Galnt3 reduced GAGs and resulted in a severe reduction of Acan in the cartilage extracellular matrix.

EXPERIMENTAL PROCEDURES

Cell Culture and Adenoviral Transfer—Primary chondrocytes were prepared from the skeletons of embryonic day 18.5 (E18.5) *Runx2*$^{-/-}$ embryos as described previously (19). Primary chondrocytes were infected with either green fluorescent protein (GFP)-expressing or *Runx2*- and GFP-expressing adenovirus as described previously (20).

Real-time RT-PCR Analysis—We prepared total RNA from cartilaginous tissues of wild-type, *Runx2*$^{-/-}$, and *Galnt3* transgenic embryos and from *Runx2*$^{-/-}$ primary chondrocytes. RNA samples were reverse transcribed using Moloney murine leukemia virus reverse transcriptase (Invitrogen). The cDNA was analyzed by real-time PCR using SYBR Green mix and the ABI7700 cycler (Applied Biosystems). Primers used for amplification were as follows: *Runx2*, CCGCACGACAACCGCACCAT and CGCTCCGGCCCACAAATCTC; *Galnt3*, ACACTATTTACCCGGAAGCG and AGCTCCTTCTGGATGTTGTG, *Ihh*, TTCAAGGACGAGGAGAACACG and TTCAGACGGTCCTTGCAGC; *Pthlh*, CAGTGGAGTGTCCTGGTATT and GATCTCCGCGATCAGATGGT; *Pth1r*, CAGGCGCAATGTGACAAGC and TTTCCCGGTGCCTTCTCTTTC; *Bmp2*, TAGATCTGTACCGCAGGCAC and CCCACTCATCTCTGGAAGTT. Primer sequences for other Galnt family members were described previously (21). *Gapdh* was used as an internal control.

Generation of Galnt3$^{-/-}$ *Mice and Galnt3 Transgenic Mice—Galnt3*$^{-/-}$ *mice* were generated as described previously (22). The background of *Galnt3*$^{-/-}$ *mice* was originally a mixed 129Ola/C57BL6 background. *Galnt3*$^{-/-}$ mice in a mixed 129Ola/C57BL6 background were backcrossed to C57BL/6 at least 14 generations prior to the analysis. To generate *Galnt3* transgenic mice, a 1902-bp mouse *Galnt3* cDNA fragment was cloned into the NotI site of a pNASSβ expression vector (Clontech), which contained the promoter and enhancer of the mouse *Col2a1* gene (23–25). The construct was injected into the pronuclei of fertilized eggs from F1 hybrid mice (C57BL/6 × C3H). Mutant embryos were identified by genomic PCR. Transgene expression was measured by real-time RT-PCR using RNA purified from the vertebrae and ribs. Serum phosphate and calcium levels were examined using the Phopha-C-test kit (Wako, Osaka, Japan) and Calcium-E-test kit (Wako), respectively. Serum testosterone levels were examined by liquid chromatography-tandem mass spectrometry (ASKA Pharma Medical Co., Ltd). Prior to the study, all experiments were reviewed and approved by the Animal Care and Use Committee of the Nagasaki University Graduate School of Biomedical Sciences.

Skeletal Examination—To evaluate the morphology of the whole skeleton, after removal of skin and internal organs, embryos at E16.5 and E18.5 were fixed in 99% ethanol for 4 days. Then the skeletons were stained with 0.015% Alcian blue 8GX and then with 0.002% alizarin red-S as described previously (26). Finally, they were cleared in an aqueous KOH solution and glycerol.

Histological Analyses—Samples were fixed in 4% paraformaldehyde, 0.1 M phosphate buffer and embedded in paraffin. Sections (7 μm thick) were stained with hematoxylin and eosin (H&E) and the von Kossa method. For *in situ* hybridization, single-stranded RNA probes were labeled with digoxigenin-11-UTP using a DIG RNA labeling kit (Roche Applied Science) according to the manufacturer's instructions. Sections were hybridized using mouse *Col2a1*, *Acan*, *Col10a1*, and *Spp1* antisense probes as described previously (17). To prepare *Galnt3* probes, cDNA fragments were inserted in pBluescript (Stratagene). The 5′- and 3′-end sequences were as follows: ATGGCTCACCTTAAGCGACT/CAAGGGTACTACACAGCCGC; GAATTCAACAAGCCTTCTCC/TAAAAATTTTACCTGGTACC, and GGTACCTGAACACTATTTAC/TTTTTAGCCAAAATGAATAA. Safranin O staining was performed as follows. After deparaffinization and hydration of tissue sections, cellular staining was achieved with Weigert's acid iron chloride hematoxylin (1%) and 0.02% fast green FCF in 1% acetic acid. Finally, sulfated proteoglycans were stained with 0.1% safranin O in distilled water for 6 min. The sections were counterstained with methyl green. For PAS staining, tissue slices were oxidized in 1% periodic acid for 10 min and rinsed several times in deionized water. Then the slides were immersed in Schiff's reagent (Merck) at room temperature for 10 min and washed in tap water for 10 min. The sections were counterstained with hematoxylin. Acan immunohistochemistry was done using rabbit polyclonal anti-aggrecan antibody (AB 1031, Chemicon, Temecula, CA) after treatment with chondroitinase ABC (Sigma). Color visualization of the target was obtained with diaminobenzidine tetrahydrochloride substrate. The sections were counterstained with methyl green.

BrdU Incorporation Study and TUNEL Staining—For BrdU incorporation experiments, 18.5-day postcoitus pregnant mice were intraperitoneally injected with 50 μg of BrdU/g of body weight. One hour later, embryos were obtained by cesarean dissection. Mice at 3 weeks of age were injected intraperitoneally with 100 μg of BrdU/g of body weight and sacrificed 1 h later. BrdU incorporation by proliferating cells was detected by immunohistochemistry using monoclonal mouse anti-BrdU antibody (Dako). Visualization was achieved by the EnVision system (Dako) and DAB (3,3′-diaminobenzidine, tetrahydrochloride) substrate. Sections were counterstained with toluidine blue. Apoptotic cells were identified in tibia sections by TUNEL staining using the ApopTag peroxidase *in situ* apoptosis detection kit (Chemicon).

Lectin Histochemistry—After blocking endogenous peroxidase activity with 0.3% H_2O_2 in methanol, sections were treated with PBS, containing 1% bovine serum albumin and 0.05% Tween 20 for 30 min and incubated with biotinylated *Vicia villosa* agglutinin (VVA) (5 μg/ml) (Vector Laboratories Inc., Burlingame, CA) at room temperature for 1 h. Then they were rinsed with PBS, incubated with horseradish peroxidase-conjugated streptavidin (2.5 μg/ml) (Vector Labs) at room temperature for 1 h, and visualized as a brown reaction product by applying Histofine Simple Stain DAB solution (Nichirei). The sections were counterstained with methyl green. The following controls for specificity of lectin labeling were used: 1) preabsorption of lectins with inhibiting sugars, *N*-acetylgalactosamine (200 mM; Vector Labs) and 2) substitution of biotinylated lectins with PBS.

Western Blot Analysis—Whole-tissue lysates were prepared from the limb skeletons at E15.5 and the epiphyses of femurs and tibiae at postnatal day 10 in 50 mM Tris-HCl (pH 7.4), 50 mM sodium acetate containing protease inhibitors (Roche Applied Science). To detect VVA reactivity, lysates were digested with 0.25 units/ml chondroitinase ABC (Sigma) at 37 °C for 2 h. Membrane blots were incubated first with biotinylated VVA (0.4 μg/ml) and then with horseradish peroxidase-conjugated streptavidin (0.1 μg/ml). To detect Acan protein, lysates were digested with 0.25 units/ml chondroitinase ABC (Sigma) or with 0.25 units/ml chondroitinase ABC, 1 unit/ml neuraminidase (New England Biolabs), and 10 units/ml *O*-glycosidase (New England Biolabs) at 37 °C for 2 h with agitation (220 rpm). Sodium chloride (final concentration 150 mM) and Triton X-100 (final concentration 1%) were added, and the lysates were agitated at 37 °C for 1 h. After centrifugation, the supernatants were used for Western blot analysis. Membrane blots were incubated first with rabbit polyclonal antibody against Acan (Chemicon) or goat polyclonal antibody against actin (Santa Cruz Biotechnology, Inc.) and then with the corresponding secondary antibodies conjugated with horseradish peroxidase.

Immunoprecipitation Assay—Whole-tissue lysates were prepared from the limb skeletons at E15.5 in 50 mM Tris-HCl (pH 7.4), 50 mM sodium acetate containing protease inhibitors (Roche Applied Science). Lysates were digested with 0.25 units/ml chondroitinase ABC at 37 °C for 2 h. After centrifugation, the supernatants were incubated with anti-Acan (1 μg) antibody (AB 1031, Chemicon) and 50 μl of Dynabeads Protein G (Invitrogen) at 4 °C overnight with rotation. The beads were washed three times in washing buffer, and immunocomplexes were analyzed by Western blotting. Membrane blots were incubated first with biotinylated VVA (0.4 μg/ml) and then with horseradish peroxidase-conjugated streptavidin (0.1 μg/ml).

Isolation of GAGs—Cartilage samples were suspended in water and boiled at 100 °C for 10 min. Borate-NaOH and $CaCl_2$ were added to a final concentration of 1 M and 10 mM, respectively. Samples were sequentially digested first with Pronase (2% (w/w) of the sample) at 60 °C for 24 h and then with actinase (1% (w/w) of the sample), which was added twice at a 24-h interval. After a total of 96 h of digestion, proteins were precipitated by adding trichloroacetic acid (TCA) at a concentration of 5%, and the mixtures were centrifuged. The precipitates were resuspended in 5% TCA and centrifuged again. The supernatants were pooled, and the excess TCA was removed by extraction with diethyl ether. GAGs were precipitated at 4 °C overnight by adding 4 volumes of 80% ethanol containing 5% sodium acetate. Finally, the precipitates were collected by centrifugation and dried.

Disaccharide Composition Analysis—An aliquot of each GAG preparation was digested with chondroitinase ABC, followed by labeling with a fluorophore, 2-aminobenzamide. Excess 2-aminobenzamide was removed with chloroform. Labeled disaccharides were diluted with 16 mM NaH_2PO_4 to a final volume of 100 μl, and an aliquot was analyzed by anion exchange HPLC on an amine-bound silica PA-03 column (YMC-Pack PA, Kyoto, Japan) by fluorescent detection (excitation and emission wavelengths at 330 and 420 nm, respectively).

Analysis of the Chain Length of Chondroitin Sulfate—The molecular mass of the chondroitin sulfate preparations was determined by gel filtration using a column of Superdex 200 calibrated with molecular mass markers, including dextran preparations (average mass, 18.1, 37.5, and 65.5 kDa) and heparan sulfate from bovine intestinal mucosa (average mass, 7.5 kDa). Two micrograms of chondroitin sulfate preparations were loaded onto the column and eluted with 0.2 M ammonium bicarbonate at a flow rate of 0.3 ml/min, and the fractions were collected at 3-min intervals, dried, and reconstituted in 50 μl of water. An aliquot (20 μl) from fraction 8 to fraction 24 was taken for chondroitin sulfate analysis using a PA-03 amine-bound silica column after chondroitinase ABC digestion followed by labeling with 2-aminobenzamide.

Statistical Analysis—Values are shown as mean ± S.D. Statistical analyses of two groups were performed by Student's *t* test, and those of three groups were performed by ANOVA and the Tukey-Kramer post hoc test. A p value of less than 0.05 was considered significant.

RESULTS

Involvement of Runx2 in Galnt3 Expression and the Expression of Galnt Family Genes during Skeletal Development—We searched Runx2 target genes by introducing *Runx2* into primary *Runx2*$^{-/-}$ chondrocytes using a microarray. *Galnt3* expression was induced 5 times by the infection of adenovirus expressing *Runx2* and GFP compared with that expressing GFP. Real-time RT-PCR analysis confirmed the induction of *Galnt3* expression by Runx2 (Fig. 1, *A* and *B*). *Galnt3* expres-

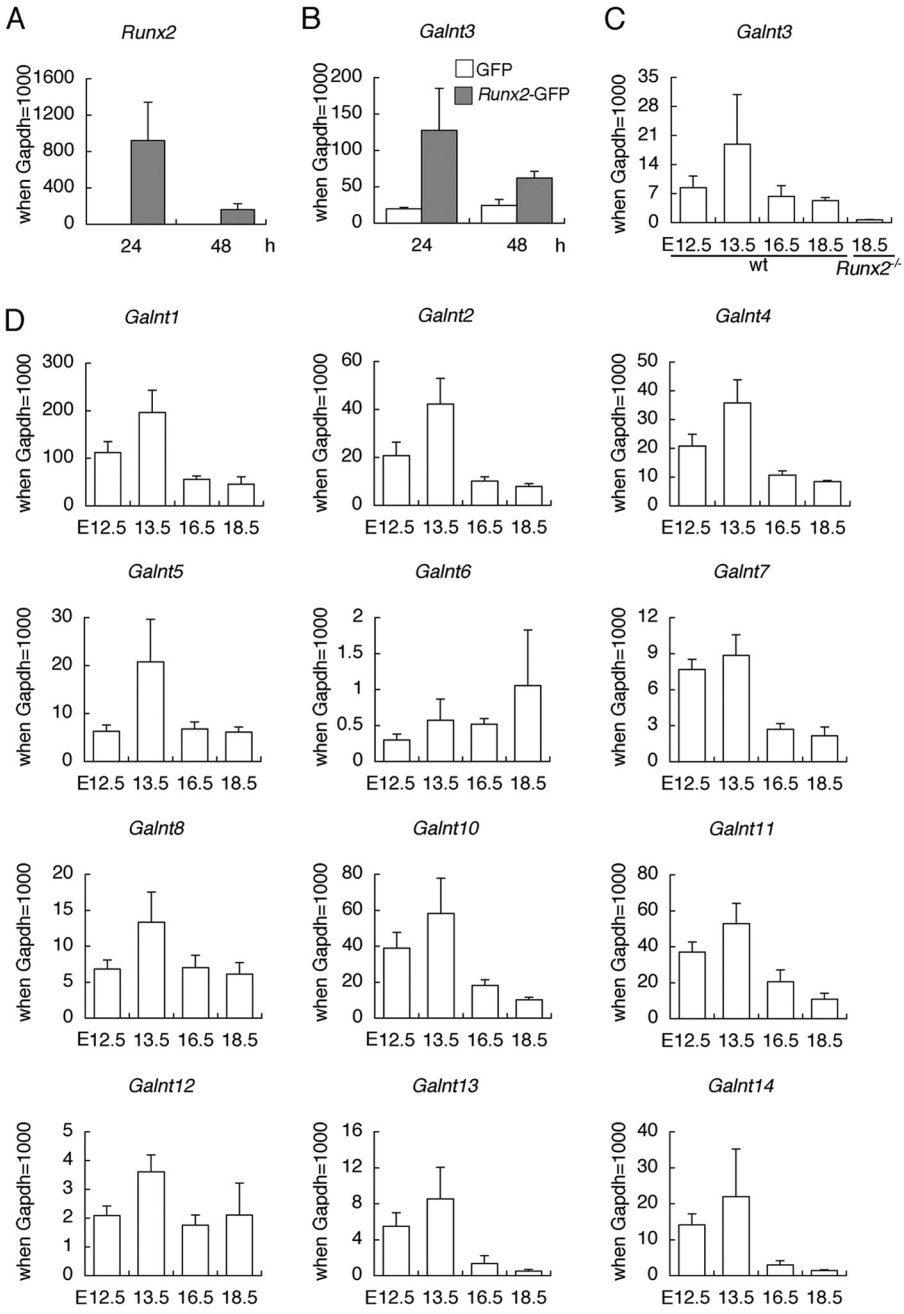

FIGURE 1. **Real-time RT-PCR analysis.** *A* and *B*, induction of *Galnt3* expression by Runx2. *Runx2*$^{-/-}$ primary chondrocytes were infected with adenovirus expressing GFP (*open columns*) or expressing *Runx2* and GFP (*closed columns*), and the expressions of *Runx2* (*A*) and *Galnt3* (*B*) were examined at 24 and 48 h after the infection. $n = 3$. *C* and *D*, *Galnt3* expression in wild-type mice at E12.5, E13.5, E16.5, and E18.5 and *Runx2*$^{-/-}$ mice at E18.5 (*C*) and the expression of Galnt family genes in wild-type mice at E12.5, E13.5, E16.5, and E18.5 (*D*). $n = 3–6$. *Gapdh* was used as an internal control, and the value of *Gapdh* was set as 1000 and the relative levels are shown. *Error bars*, S.D.

sion in skeletal tissues was examined in wild-type mice at E12.5, E13.5, E16.5, and E18.5 and in *Runx2*$^{-/-}$ mice at E18.5. *Galnt3* expression was highest at E13.5 in wild-type mice, and it was severely reduced in *Runx2*$^{-/-}$ mice at E18.5, when the skeletons are cartilaginous (Fig. 1*C*). The expression of Galnt family genes in skeletal tissues of wild-type mice was also examined (Fig. 1*D*). Many Galnt family genes, including *Galnt1*, *Galnt2*, *Galnt4*, *Galnt5*, *Galnt8*, *Galnt10*, *Galnt11*, and *Galnt14*, were also expressed at levels similar to or higher than that of *Galnt3*, with the highest level at E13.5, when the skeletons are cartilaginous. These findings indicate that *Galnt3* expression is regulated by Runx2 in chondrocytes, but many Galnt family genes are redundantly expressed in cartilaginous tissues. To clarify the function of Galnt3 in chondrocytes, we generated *Galnt3*$^{-/-}$ mice and chondrocyte-specific *Galnt3* transgenic mice.

Galnt3$^{-/-}$ *Mice Showed a Delay in Endochondral Ossification at E16.5*—We examined the skeletal development of *Galnt3*$^{-/-}$ embryos at E16.5. *Galnt3*$^{-/-}$ mice showed mild dwarfism, and the lengths of limb skeletons were shortened (Fig. 2, *A–K*). The lengths of mineralized area in the humeri of *Galnt3*$^{-/-}$ embryos were significantly shorter than those of wild-type and *Galnt3*$^{+/-}$ embryos (Fig. 2*L*), indicating that the

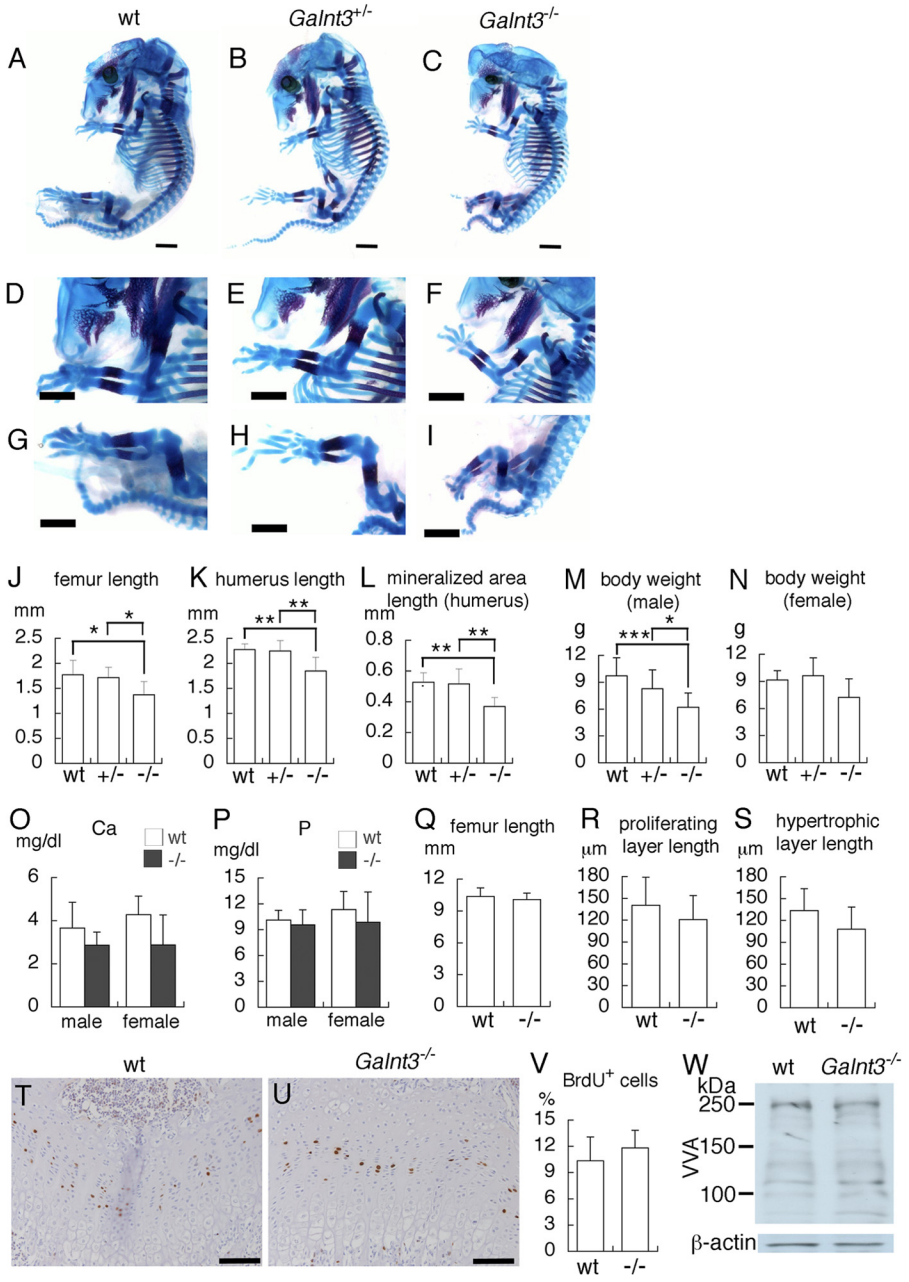

FIGURE 2. **Phenotypes of *Galnt3*$^{-/-}$ mice.** *A–L*, skeletal examination at E16.5. Lateral views of whole embryos (*A–C*), forelimbs (*D–F*), and hind limbs (*G–I*) of wild-type (*A*, *D*, and *G*), *Galnt3*$^{+/-}$ (*B*, *E*, and *H*), and *Galnt3*$^{-/-}$ (*C*, *F*, and *I*) embryos. The lengths of femurs (*J*), humeri (*K*), and the mineralized area of humeri (*L*) in wild-type ($n = 8$), *Galnt3*$^{+/-}$ ($n = 11$), and *Galnt3*$^{-/-}$ ($n = 6$) embryos were measured. *M–V*, analyses of mice at 3 weeks of age. *M*, body weight of wild-type ($n = 18$), *Galnt3*$^{+/-}$ ($n = 26$), and *Galnt3*$^{-/-}$ ($n = 11$) male mice. *N*, body weight of wild-type ($n = 10$), *Galnt3*$^{+/-}$ ($n = 24$), and *Galnt3*$^{-/-}$ ($n = 9$) female mice. *O* and *P*, serum concentration of calcium (*O*) and phosphate (*P*) in wild-type (male, $n = 11$; female, $n = 5$) and *Galnt3*$^{-/-}$ (male, $n = 3$; female, $n = 5$) mice. *Q–S*, the lengths of femurs (*Q*) and lengths of proliferating (*R*) and hypertrophic (*S*) layers in wild-type ($n = 10$) and *Galnt3*$^{-/-}$ ($n = 10$) male mice. The lengths of proliferating and hypertrophic chondrocyte layers were measured using H&E-stained sections. *T–V*, BrdU staining of wild-type (*T*) and *Galnt3*$^{-/-}$ (*U*) male mice and the frequencies of BrdU-positive cells in the growth plates of femurs in wild-type ($n = 5$) and *Galnt3*$^{-/-}$ ($n = 5$) male mice (*V*). *W*, reactivity to VVA. Lysates, which were prepared from the epiphyses of femurs and tibiae at postnatal day 10, were treated with chondroitinase ABC. The membrane was reacted with VVA or exposed to anti-β-actin antibody. Similar results were obtained in four wild-type and four *Galnt3*$^{-/-}$ mice, and representative data are shown. *, $p < 0.05$; **, $p < 0.01$; ***, $p < 0.001$. *Scale bars*, 1 mm (*A–I*) and 100 μm (*T* and *U*). *Error bars*, S.D.

process of endochondral ossification is retarded. At 3 weeks of age, the body weights of *Galnt3*$^{-/-}$ male mice but not *Galnt3*$^{-/-}$ female mice were significantly lower than those of wild-type and *Galnt3*$^{+/-}$ mice of the respective sex (Fig. 2, *M* and *N*). There was no significant difference in serum testosterone levels between wild-type and *Galnt3*$^{-/-}$ male mice (wild type, 20.9 ± 6.2 pg/ml, $n = 18$; *Galnt3*$^{-/-}$, 16.6 ± 6.2 pg/ml, $n = 7$). The serum concentrations of calcium and phosphate were similar between wild-type and *Galnt3*$^{-/-}$ mice in both sexes (Fig. 2, *O* and *P*). The lengths of femurs and the lengths of proliferating chondrocyte layers and hypertrophic chondrocyte layers were similar between wild-type and *Galnt3*$^{-/-}$ male mice (Fig. 2, *Q* and *S*). Further, there was no difference in the frequencies of BrdU-positive cells between wild-type and *Galnt3*$^{-/-}$ male mice (Fig. 2, *T–V*). In order to examine the presence of mucin-type *O*-glycans in growth plates, the reac-

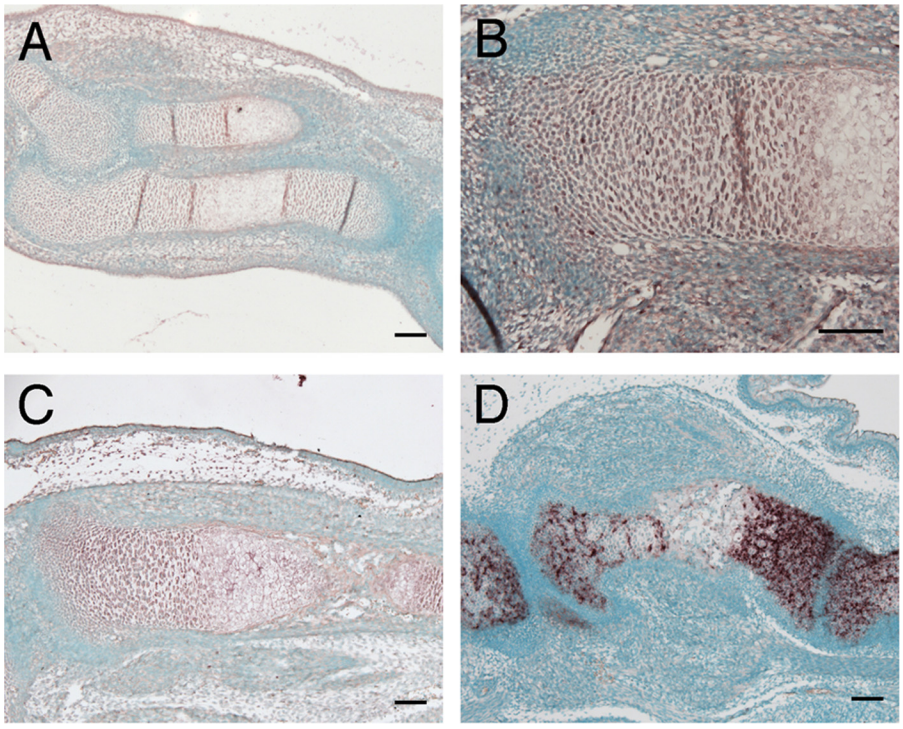

FIGURE 3. ***In situ* hybridization of *Galnt3* mRNA.** Shown is *in situ* hybridization of *Galnt3* mRNA using sections of wild-type forelimb at E13.5 (*A*) and tibia at E14.5 (*B*) and E15.5 (*C*) and *Galnt3* transgenic tibia at E16.5 (*D*). *Scale bars*, 100 μm.

tivity to VVA, which recognizes the Tn antigen (GalNAc-*O*-Ser/Thr) generated by GalNAc-transferase (27, 28), was examined. Lysates from wild-type and *Galnt3*$^{-/-}$ mice showed a similar level of VVA reactivity (Fig. 2*W*), probably due to the redundant expression of Galnt family genes in growth plates (Fig. 1*D*).

Galnt3 Overexpression in Cartilage Resulted in Skeletal Abnormalities—In wild-type mice, *Galnt3* was expressed in resting, proliferating, and prehypertrophic chondrocytes (Fig. 3, *A*–*C*). To examine the function of Galnt3 in chondrocytes, we generated chondrocyte-specific *Galnt3* transgenic mice under the control of the *Col2a1* promoter-enhancer, which directs transgene expression to resting, proliferating, and prehypertrophic chondrocytes. In *Galnt3* transgenic mice, *Galnt3* was strongly detected in resting, proliferating, and prehypertrophic chondrocytes (Fig. 3*D*).

Galnt3 transgenic mice survived until delivery but died just after birth. Therefore, we analyzed F_0 transgenic mice at the embryonic stage (Table 1). Macroscopically, transgenic embryos displayed severe dwarfism, domed skulls, short limbs and mandible, protruding tongue, and cleft palate (Table 1) (Fig. 4, *A* and *B*). All of the *Galnt3* transgenic embryos with dwarfism expressed the transgene in cartilage, and the levels of the transgene expression were correlated with the severity of dwarfism. Skeletal staining of embryos at E18.5 with alizarin red and Alcian blue revealed that *Galnt3* transgenic mice had shorter or smaller endochondral bones than wild-type siblings. The small sternum and ribs resulted in bell-shaped thoracic cages (Fig. 4*C*). As expected, bones derived from intramembranous ossification were similarly mineralized in wild-type and *Galnt3* transgenic mice (Fig. 4*C*).

TABLE 1
Production frequency of transgenic mice

Age	Obtained mice	Transgenic mice	Transgenic mice with dwarfism
E13.5	48	6	Not distinguishable
E14.5	79	8	6
E15.5	605	80	47
E16.5	183	44	24
E17.5	27	8	3
E18.5	416	83	46

Galnt3 Transgenic Mice Displayed a Disorganized Growth Plate—Wild-type growth plates at E16.5 and E18.5 showed chondrocytes arranged in morphologically distinguishable layers: resting, proliferating, hypertrophic, and terminal hypertrophic chondrocyte layers (Fig. 5, *A*, *C*, *E*, and *G*). In the resting chondrocyte layer, chondrocytes were small, round, and uniformly scattered. In the proliferating chondrocyte layer, they became flattened and arranged themselves in groups of columns that were oriented parallel to the longitudinal axis of the bone. With further differentiation, the chondrocytes gradually increased in size and established the hypertrophic chondrocyte layer. Terminal differentiation resulted in mineralization of the extracellular matrix around the terminal hypertrophic chondrocytes (Fig. 5, *A*, *C*, *E*, and *G*).

In contrast, *Galnt3* transgenic mice with high transgene expression had disorganized growth plates. Each chondrocyte layer except the terminal hypertrophic chondrocyte layer was short compared with the respective layer in wild-type mice, and the separation between layers was not clear (Fig. 5, *B*, *D*, *F*, and *H*). In the resting chondrocyte layer, chondrocytes were present at a high density, surrounded by scarce extracellular matrix (Fig. 5, *D* and *H*). The proliferating chondrocyte layer contained round chondrocytes mixed with flattened chondrocytes, and

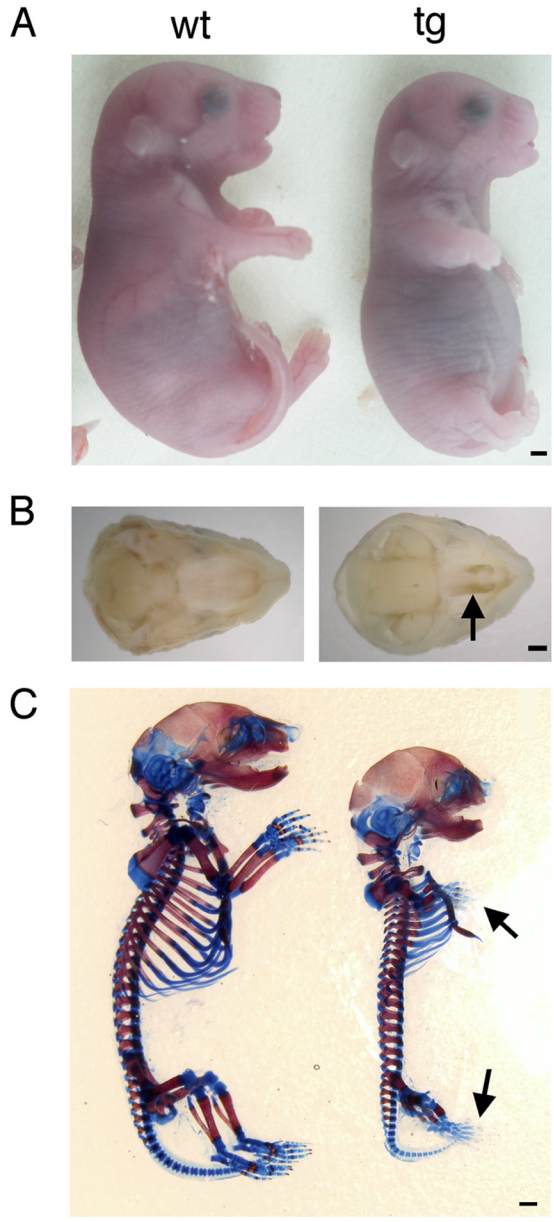

FIGURE 4. **Appearance and skeletal system of *Galnt3* transgenic embryos.** *A*, macroscopic appearance of wild-type (*wt*) and *Galnt3* transgenic (*tg*) embryos at E18.5. The abdomen in *Galnt3* transgenic embryos was protruded because of the small thoracic cage. *B*, macroscopic views of the palates of wild-type (*left*) and *Galnt3* transgenic (*right*) embryos at E18.5. A *Galnt3* transgenic embryo presents cleft palate (*arrow*). *C*, skeletons of wild-type (*left*) and *Galnt3* transgenic (*right*) embryos at E18.5 stained with alizarin red and Alcian blue. The *arrows* indicate the reduced Alcian blue staining and the lack of alizarin red staining in the bones of the hand and foot. *Scale bars*, 1 mm.

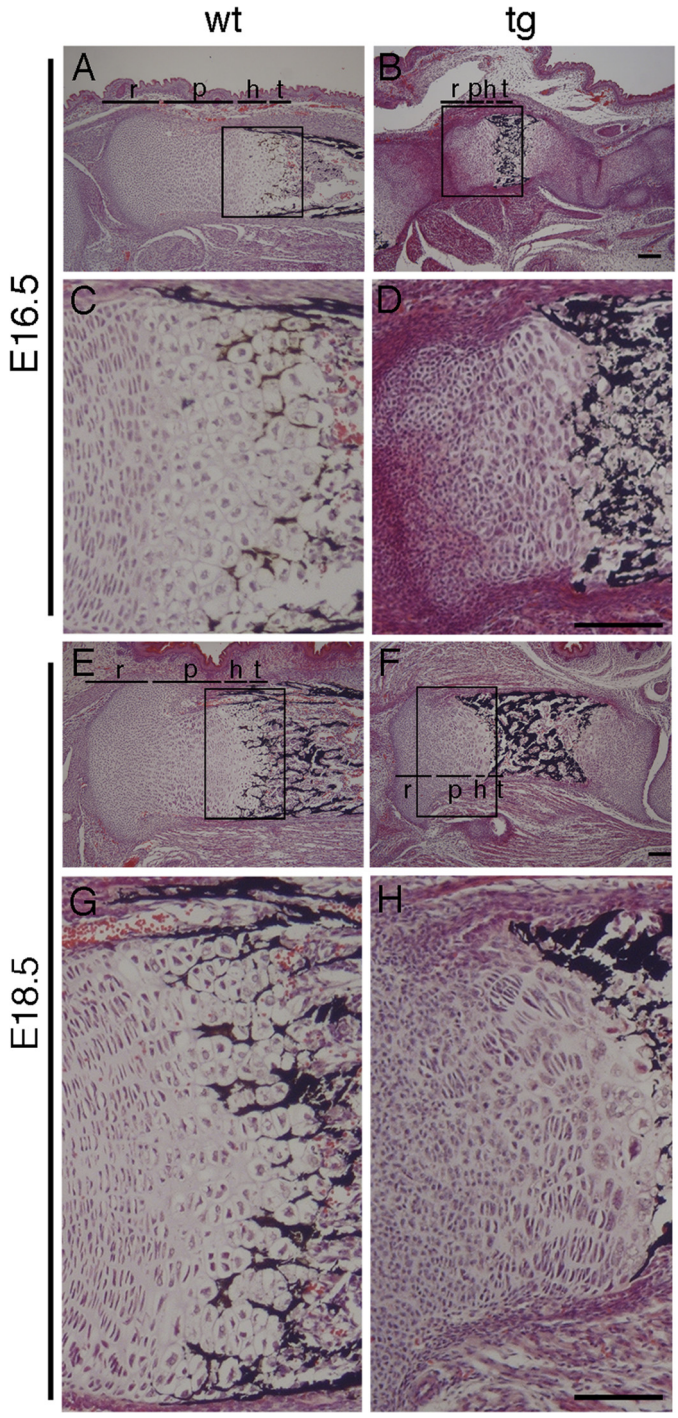

FIGURE 5. **Histological analysis of growth plates.** H&E and von Kossa staining of tibia sections at E16.5 (*A–D*) and E18.5 (*E–H*) from wild-type (*A*, *C*, *E*, and *G*) and *Galnt3* transgenic mice (*B*, *D*, *F*, and *H*). *Boxed regions* in *A*, *B*, *E*, and *F* are *magnified* in *C*, *D*, *G*, and *H*, respectively. The layers of resting (*r*), proliferating (*p*), hypertrophic (*h*), and terminal hypertrophic (*t*) chondrocytes are shown in *A*, *B*, *E*, and *F*. *Scale bars*, 100 μm.

the oriented columnar organization was disturbed (Fig. 5, *D* and *H*). The hypertrophic chondrocyte layer was extremely narrow (Fig. 5, *B* and *F*). The cell density was extremely high in the zone between the tibia and femur, and the boundary between joint connective tissue and the epiphyses was not clear at E16.5 (Fig. 5, *B* and *D*).

Chondrocyte Hypertrophy Was Delayed in Galnt3 Transgenic Mice—To further study the differentiation state of chondrocytes in *Galnt3* transgenic mice, we assessed the expression of *Col2a1*, *Acan*, *Col10a1*, and *Spp1* by *in situ* hybridization using metatarsal bone slices at E18.5. *Col2a1* and *Acan*, which are strongly expressed in resting and proliferating chondrocytes, were detected in the epiphysis and metaphysis; *Col10a1*, which is expressed in hypertrophic chondrocytes, was detected in the metaphysis; and *Spp1*, which is expressed in terminal hypertrophic chondrocytes, was detected in the diaphysis in wild-type embryos (Fig. 6, *A*, *C*, *E*, and *G*). In *Galnt3* transgenic mice,

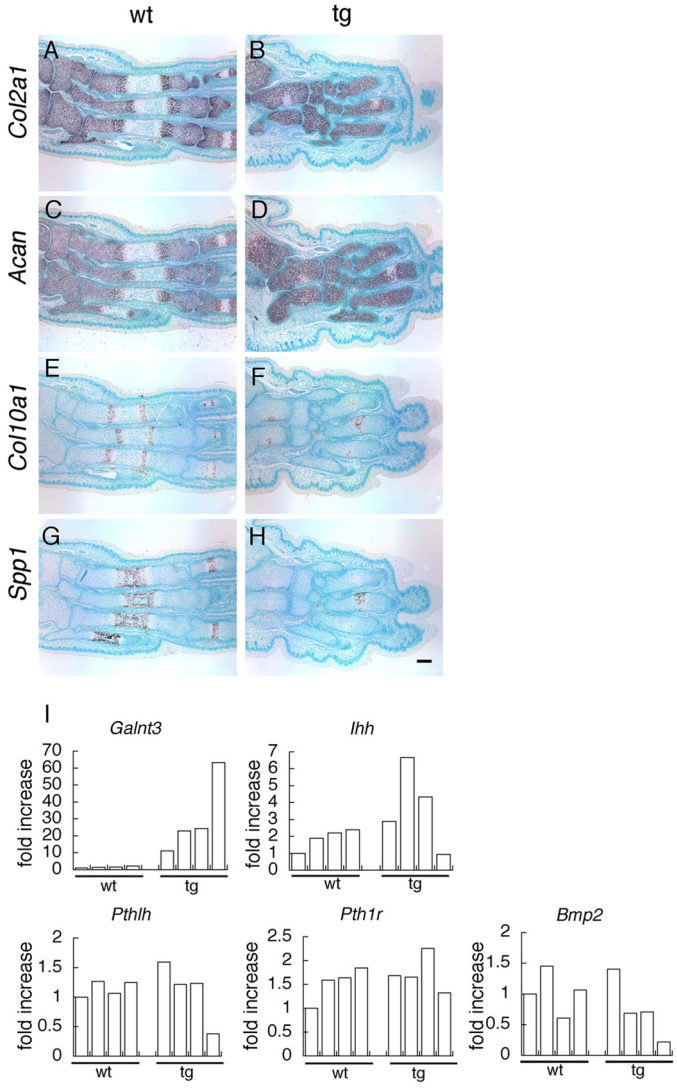

FIGURE 6. ***In situ* hybridization and real-time RT-PCR analysis.** Shown is *in situ* hybridization of sections of tarsal and metatarsal bones from wild-type (*A*, *C*, *E*, and *G*) and *Galnt3* transgenic (*B*, *D*, *F*, and *H*) embryos at E18.5 using *Col2a1* (*A* and *B*), *Acan* (*C* and *D*), *Col10a1* (*E* and *F*), and *Spp1* (*G* and *H*) antisense probes. We detected no signal using sense probes (data not shown). *Scale bar*, 100 μm. *I*, real-time RT-PCR analysis of *Galnt3*, *Ihh*, *Pthlh*, *Pth1r*, and *Bmp2*. RNA was extracted from the cartilaginous tissues of four wild-type and four F_0 *Galnt3* transgenic embryos at E15.5.

however, *Col2a1* and *Acan* were detected in most parts of the metatarsal bones, and *Col10a1* and *Spp1* expression were restricted to the center of the diaphysis, indicating that chondrocyte hypertrophy was delayed in *Galnt3* transgenic mice (Fig. 6, *B*, *D*, *F*, and *H*).

We examined the expression of *Galnt3*, *Ihh*, *Pthlh*, *Pth1r*, and *Bmp2* by real-time RT-PCR using the RNA from cartilaginous tissues of four wild-type and four F_0 *Galnt3* transgenic embryos at E15.5 (Fig. 6*I*). *Ihh* expression was up-regulated in *Galnt3* transgenic embryos with medial transgene expression but down-regulated in *Galnt3* transgenic embryo with high transgene expression. *Pthlh* expression was down-regulated in *Galnt3* transgenic embryo with high transgene expression. The levels of *Bmp2* expression were inversely correlated with those of transgene expression.

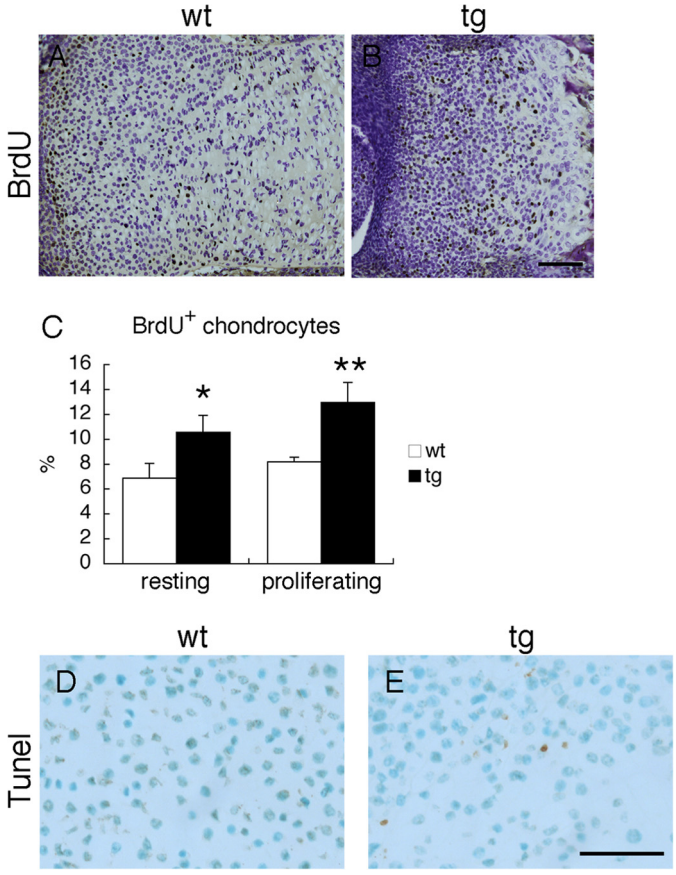

FIGURE 7. **BrdU labeling and TUNEL staining.** *A* and *B*, immunolocalization of incorporated BrdU on tibia slices from wild-type (*A*) and *Galnt3* transgenic (*B*) embryos at E18.5. *Scale bar*, 100 μm. *C*, the percentage of BrdU-positive cells in wild-type (*wt*) and *Galnt3* transgenic (*tg*) mice. The percentage was analyzed in the resting and proliferating layers. The cells in a minimum of three sections per embryo were counted, and three wild-type and three *Galnt3* transgenic embryos were examined. *, $p < 0.05$; **, $p < 0.001$. *D* and *E*, TUNEL staining of resting chondrocyte layers from wild-type (*D*) and *Galnt3* transgenic (*E*) embryos at E18.5. *Scale bar*, 50 μm. *Error bars*, S.D.

Increased Proliferation and Apoptosis in Chondrocytes of Galnt3 Transgenic Mice—To understand whether abnormal cell proliferation and/or apoptosis contributed to the dwarfism in *Galnt3* transgenic mice, we performed BrdU incorporation experiments and TUNEL staining using sections of tibias at E18.5. The growth plates in *Galnt3* transgenic mice showed increased percentages of cells incorporating BrdU compared with wild-type mice (Fig. 7, *A*–*C*). On TUNEL staining, the growth plates in both wild-type and *Galnt3* transgenic mice showed several apoptotic cells in the terminal hypertrophic chondrocyte layers (data not shown). However, the growth plates in *Galnt3* transgenic mice also displayed abnormal apoptotic cells in the resting and proliferating layers (Fig. 7, *D* and *E*).

Increase in Tn Antigen and Enhanced PAS Staining but Decrease in GAGs in the Growth Plates of Galnt3 Transgenic Mice—VVA binding was detected in resting, proliferating, and prehypertrophic chondrocytes with strongest intensity in the proliferating chondrocytes in metatarsal bones of wild-type mice at E18.5, whereas it was more strongly detected in many of the chondrocytes in *Galnt3* transgenic mice (Fig. 8, *A* and *B*). To evaluate the cartilage extracellular matrix, the serial sections were stained with safranin O, which detects sulfated GAGs. It

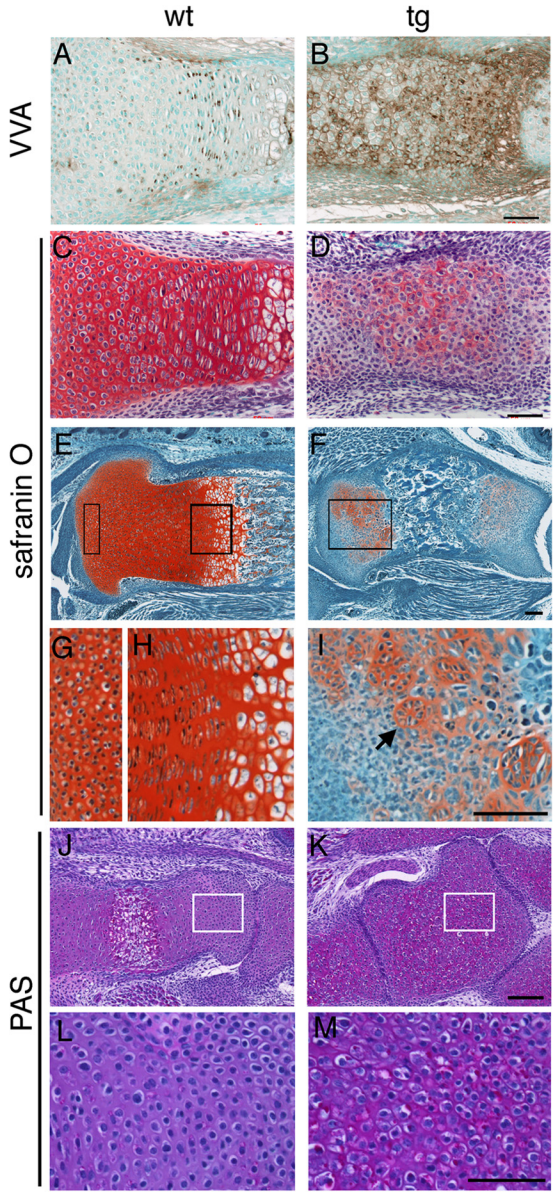

FIGURE 8. **Lectin histochemistry and safranin O and PAS staining.** *A* and *B*, VVA histochemistry. VVA-binding was examined using sections of metatarsal bones from wild-type (*A*) and *Galnt3* transgenic (*B*) embryos at E18.5. *C* and *D*, the serial sections of *A* and *B* were stained with safranin O. *E–I*, safranin O staining of sections of tibiae from wild-type (*E*, *G*, and *H*) and *Galnt3* transgenic (*F* and *I*) embryos at E18.5. The *two boxed regions* in *E* are *magnified* in *G* and *H*, and the *boxed region* in *F* is *magnified* in *I*. The *arrow* in *I* indicates a group of chondrocytes disposed in a round-shaped cluster instead of a columnar form. *J–M*, PAS staining of sections of calcanei from wild-type (*J* and *L*) and *Galnt3* transgenic (*K* and *M*) embryos at E18.5. The *boxed regions* in *J* and *K* are *magnified* in *L* and *M*, respectively. *Scale bars*, 50 μm (*A–D*, *L*, and *M*) and 100 μm (*E–K*).

stained cartilage extracellular matrix strongly and uniformly in the wild-type section, whereas it seemed to stain the extracellular matrix in a reciprocal manner with VVA in the *Galnt3* transgenic section (Fig. 8, *C* and *D*). In the sections from tibiae of *Galnt3* transgenic mice, safranin O failed to stain the periarticular region, and the staining was uneven and much weaker than in wild-type mice in the rest of the growth plates (Fig. 8, *E–I*). We observed the reduction in safranin O staining as early as E14.0 (data not shown).

Oligosaccharides and molecules with carbohydrate glycol groups with neutral electrostatic charge, such as glycoproteins and glycolipids, but not acidic GAGs, which contain negatively charged disaccharides, are stained with standard periodic acid-Schiff (PAS) (29). Using the classic short time oxidation reaction, sections of calcanei at E18.5 were stained with PAS. The staining was detected in resting, proliferating, and hypertrophic chondrocytes with the strongest intensity in the hypertrophic chondrocytes, but the staining in the extracellular matrix was weak in wild-type mice. In *Galnt3* transgenic mice, it was strongly detected in most of the chondrocytes and in the extracellular matrix (Fig. 8, *J–M*).

Aggrecan Protein but Not mRNA Was Severely Reduced in the Growth Plates of Galnt3 Transgenic Mice—Because GAGs were reduced in the growth plates of *Galnt3* transgenic mice, we examined the mRNA and protein distribution of Acan, the most abundant proteoglycan, by *in situ* hybridization and immunohistochemistry, respectively. *Acan* mRNA was strongly expressed in the resting, proliferating, and prehypertrophic chondrocyte layers in the growth plates of wild-type and *Galnt3* transgenic mice (Fig. 9, *A* and *B*). Acan protein was strongly detected in the resting, proliferating, prehypertrophic, and hypertrophic chondrocyte layers of wild-type mice, whereas it was only detected in a striped pattern and was virtually depleted in many areas in *Galnt3* transgenic mice (Fig. 9, *C–G*). The degree of the reduction in Acan protein was dependent on the transgene expression level. In *Galnt3* transgenic mice with high transgene expression, the reduction in Acan protein was extended to all chondrocyte layers (Fig. 9, *C–G*), whereas it was restricted to the resting chondrocyte layer in *Galnt3* transgenic mice with low transgene expression (Fig. 9, *H–J*). The reverse relation of the levels of Acan protein and the transgene expression was also observed in the other five F_0 transgenic mice, which were examined by immunohistochemistry (data not shown). To compare the amount of Acan protein, lysates were digested with chondroitinase ABC or with chondroitinase ABC, neuraminidase, and *O*-glycosidase and examined by Western blotting. In both methods, Acan protein was reduced in *Galnt3* transgenic mice compared with wild-type mice in a manner dependent on the levels of transgene expression (Fig. 9, *K* and *L*). To examine the VVA reactivity in Acan protein, lysates treated with chondroitinase ABC were immunoprecipitated with Acan antibody, and the immunoprecipitated protein was reacted with VVA (Fig. 9*M*). VVA reactivity in Acan protein was greatly enhanced in *Galnt3* transgenic mice compared with wild-type mice.

Chondroitin Sulfate Was Reduced but the Elongation of Chondroitin Sulfate Repeats Was Not Severely Disturbed in the Cartilage of Galnt3 Transgenic Mice—Chondroitin sulfate is the predominant GAG attached to Acan. There are several types of chondroitin sulfate with sulfation at different positions. We quantified total chondroitin sulfate disaccharides, non-sulfated chondroitin disaccharides, chondroitin 4-sulfate disaccharides, and chondroitin 6-sulfate disaccharides in cartilage samples at E15.5. The levels of all of them were reduced in *Galnt3* transgenic mice compared with wild-type mice (Fig. 10, *A–D*). Chondroitin sulfate disaccharides with

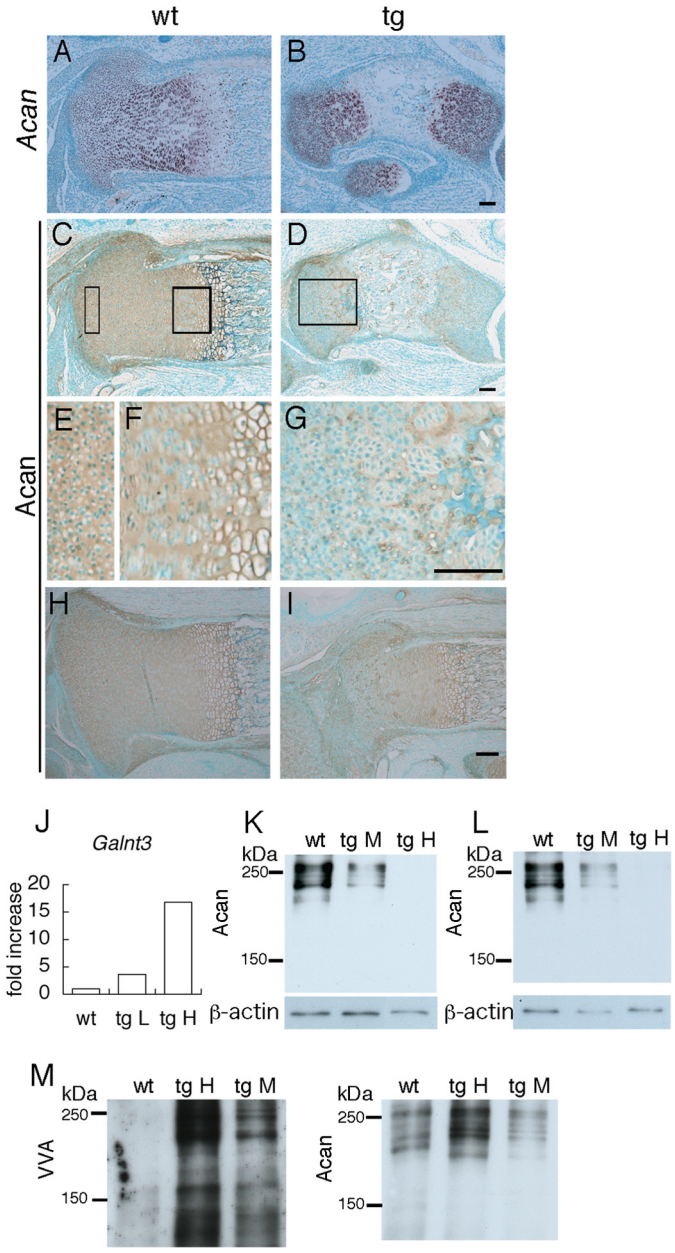

FIGURE 9. ***In situ* hybridization, immunohistochemistry, Western blot, and immunoprecipitation.** *A* and *B*, *in situ* hybridization of *Acan* mRNA in tibiae from wild-type (*A*) and *Galnt3* transgenic (*B*) embryos at E18.5. *C–I*, Acan core protein immunostaining on tibia sections from wild-type (*C*, *E*, *F*, and *H*) and *Galnt3* transgenic (*D*, *G*, and *I*) embryos at E18.5. The *two boxed regions* in *C* are *magnified* in *E* and *F*, and the *boxed region* in *D* is *magnified* in *G*. *Scale bars*, 100 μm. *J*, real-time RT-PCR analysis. *Galnt3* expression in a wild-type mouse at E18.5, a *Galnt3* transgenic mouse with low transgene expression shown in *I* (*tg L*), and a *Galnt3* transgenic mouse with high transgene expression shown in *B*, *D*, and *G* (*tg H*) is shown. The value in the wild-type mouse was set as 1, and relative levels are shown. *K* and *L*, Western blots of proteins extracted from the cartilaginous skeletons of wild-type, *Galnt3* transgenic embryo with medial transgene expression (*tg M*) and *Galnt3* transgenic embryo with high transgene expression (*tg H*) at E15.5. Lysates were digested with chondroitinase ABC (*K*) or with chondroitinase ABC, neuraminidase, and *O*-glycosidase (*L*). Membranes were exposed to anti-Acan (*top*) and anti-actin (*bottom*) antibodies. *M*, VVA reactivity of Acan. Lysate treated with chondroitinase ABC was immunoprecipitated by anti-Acan antibody. The membrane was reacted with VVA or exposed to anti-Acan antibody.

sulfation at two positions were present at very low levels in both wild-type and *Galnt3* transgenic mice (data not shown).

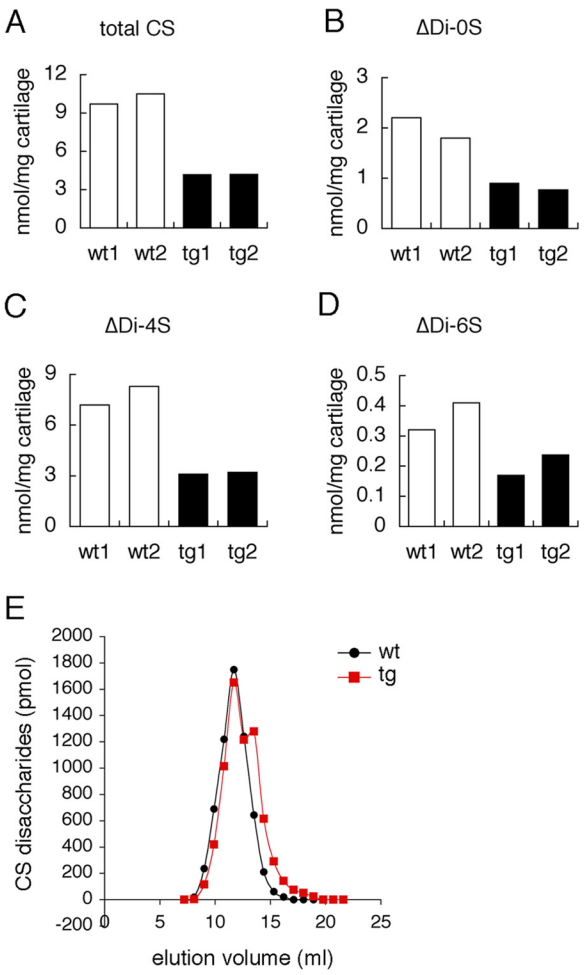

FIGURE 10. **Quantification of chondroitin sulfate disaccharides in isolated GAGs from cartilaginous skeletons.** *A–D*, chondroitin sulfate disaccharide content in isolated GAGs from cartilaginous skeletons of wild-type (*wt1* and *wt2*) and *Galnt3* transgenic (*tg1* and *tg2*) embryos at E15.5. *CS*, chondroitin sulfate; *ΔDi-0S*, non-sulfated chondroitin; *ΔDi-4S*, chondroitin 4-sulfate; *ΔDi-6S*, chondroitin 6-sulfate. *E*, chondroitin sulfate chain length analysis. Chondroitin sulfate disaccharide content in the fractionated GAGs isolated from cartilaginous skeletons of wild-type (*wt*) and *Galnt3* transgenic (*tg*) embryos at E15.5 was quantitated.

We quantitated chondroitin sulfate disaccharides after fractionation of GAGs, which had been isolated from cartilaginous skeletons at E15.5. The fractionated GAGs with higher molecular weight (fractions 10–12) contained lower amounts of chondroitin sulfate disaccharides, and the fractionated GAGs with lower molecular weight (fractions 15–19) contained higher amounts of chondroitin sulfate disaccharides in *Galnt3* transgenic mice compared with the respective sample in wild-type mice. However, both samples from wild-type and *Galnt3* transgenic mice showed the largest peak in the same fraction (fraction 13), which contained GAGs with a molecular mass of 47 kDa, and contained a similar amount of chondroitin sulfate disaccharides (Fig. 10*E*). These findings indicate that the elongation of chondroitin sulfate repeats was not severely disturbed in *Galnt3* transgenic mice.

DISCUSSION

Runx2 is an essential transcription factor for chondrocyte maturation (17, 18). We found that *Galnt3* is one of the down-

stream genes of Runx2 in chondrocytes. Although many Galnt family genes were expressed in cartilaginous tissues, *Galnt3*$^{-/-}$ mice showed dwarfism and had shortened limbs at E16.5. However, *Galnt3*$^{-/-}$ mice at 3 weeks of age had no apparent phenotypes in the growth plates, probably due to the rescue by the factors from bone marrow cells after invasion of blood vessels into the cartilage. Because the reduction in the length of mineralized area of the humeri at E16.5 indicates the retarded chondrocyte maturation, the delay in chondrocyte maturation is likely to be the reason for the shortened limbs at E16.5. Therefore, it is suggested that Galnt3 has a non-redundant function in chondrocyte maturation.

In *Galnt3* transgenic mice, endochondral bones were shortened due to the deceleration of chondrocyte hypertrophy and reduced extracellular matrix, and the growth plates were disorganized. The cell cycle was accelerated, as shown by the increased BrdU uptake, but apoptosis was also increased. The level of Tn antigen was increased, and PAS staining of extracellular matrix was enhanced, but the amount of GAGs was reduced. Further, Tn antigen was increased, but GAGs were reduced in a major proteoglycan, Acan. The protein level of Acan was reduced, depending on the level of transgene expression, although *Acan* mRNA expression was not inhibited. These findings indicate that the phenotypes described above were caused, at least in part, by the increase of mucin-type *O*-glycans and the reduction of GAGs in Acan and also indicate that the enhanced mucin-type *O*-glycosylation reduced the amount of GAGs in Acan, leading to the reduction of Acan in the extracellular matrix.

Chondroitin sulfate chains are composed of sulfated disaccharide repeats of GalNAc and D-glucuronic acid (GlcUA). Chondroitin sulfate chains are attached to core proteins like Acan, through a tetrasaccharide linker. First, xylose is *O*-linked to a serine residue by a xylosyltransferase. Then two galactose residues and a glucuronic acid residue are added by the corresponding transferases to complete the linker. Synthesis of chondroitin sulfate starts with the transfer of a GalNAc residue to the tetrasaccharide linker. Chain elongation proceeds with the alternate addition of GlcUA and GalNAc residues in coordination with sulfation (4, 8). One possible mechanism behind the reduction of GAGs in Acan is that in the Golgi apparatus, where glycosylation by xylosyltransferases and Galnt3 occurs, Galnt3 competes with xylosyltransferases for serine residues on the core protein. As suggested by Gerlitz *et al.* (30), the addition of GalNAc to serine residues could prevent assemblage of the tetrasaccharide (GlcUAb1–3Galb1–3Galb1–4Xyl) linker and consequently the synthesis of chondroitin sulfate. This idea is also compatible with the finding that the level of chondroitin sulfate was reduced but the elongation of chondroitin sulfate chain was not severely impaired in *Galn3* transgenic mice, because if the first step by xylosyltransferase is completed, the synthesis of chondroitin sulfate will proceed normally.

The secretion of Acan in *Galnt3* transgenic mice could be compromised by the defective glycosylation, because the lack of chondroitin sulfate chain attachment to the core protein inhibits Acan secretion to the extracellular matrix (31, 32), and Acan core proteins that are insufficiently glycosylated may have accumulated in the smooth endoplasmic reticulum subcompartment, where they would undergo further degradation (33). Increased extracellular breakdown could also be the reason for the reduced amounts of Acan proteoglycan in the extracellular matrix. Indeed, mice deficient in CSGalNAcT1, an enzyme that participates in chondroitin sulfate synthesis, have reduced amounts of chondroitin sulfate and also reduced amounts of Acan core protein due to augmented degradation (34).

Galnt3 yields mucin-type *O*-glycosylated proteins, which are known to play important roles in cell adhesion (35), signal transduction (36, 37), protein trafficking (38, 39), and cell proliferation, apoptosis, and cancer (40–42). They also protect proteins from protease degradation (43–45). Therefore, the phenotype of *Galnt3* transgenic mice should have been caused not only by the reduced amount of GAGs but also by the increased amount of mucin-type *O*-glycans. The expression of *Ihh* was increased in *Galnt3* transgenic mice with medial transgene expression. It may have contributed to the increase of BrdU labeling in *Galnt3* transgenic mice, because Ihh enhances chondrocyte proliferation (46). The decrease of *Ihh* expression in *Galnt3* transgenic mouse with high transgene expression may be due to the severe inhibition of chondrocyte maturation, because *Ihh* is expressed in prehypertrophic chondrocytes. The reduction of *Ihh* expression may have reduced *Pthlh* expression, because Ihh regulates *Prhlh* expression (47). The levels of *Bmp2* expression were inversely correlated with those of transgene expression. Therefore, the reduction of *Bmp2* expression may have contributed to the delay in chondrocyte maturation in *Galnt3* transgenic mice because Bmp2 plays a crucial role in chondrocyte maturation (48).

Overexpression of *Galnt3* increased mucin-type *O*-glycosylation but reduced GAGs, probably due to competition with xylosyltransferases. Because many Galnt family proteins are expressed in chondrocytes, modification of protein glycosylation by competition of Galnt family proteins with xylosyltransferases may play an important role in the physiological functions of chondrocytes. Because keratan sulfate chains are added to mucin-type *O*-sugar chains (49), the mucin-type *O*-glycosylation will also increase keratan sulfate chains in Acan. Because many Galnt family genes showed a similar expression pattern with *Galnt3* in cartilaginous tissues with the highest expression at E13.5, Galnt family proteins may modify Acan glycosylation during chondrocyte maturation. Galnt3 is also likely to regulate chondrocyte maturation, probably by specifically modifying the glycosylation of unknown proteins. Although the physiological meaning of mucin-type *O*-glycosylation of Acan has not been examined, our findings suggest that Galnt family proteins regulate chondrocyte proliferation and maturation by modifying the glycosylation of Acan.

REFERENCES

1. Lefebvre, V., and Bhattaram, P. (2010) Vertebrate skeletogenesis. *Curr. Top. Dev. Biol.* **90,** 291–317
2. Zhao, Q., Eberspaecher, H., Lefebvre, V., and De Crombrugghe, B. (1997) Parallel expression of Sox9 and Col2a1 in cells undergoing chondrogenesis. *Dev. Dyn.* **209,** 377–386
3. Gentili, C., and Cancedda, R. (2009) Cartilage and bone extracellular matrix. *Curr. Pharm. Des.* **15,** 1334–1348
4. Varki, A., Cummings, R. D., Esko, J. D., Freeze, H. H., Stanley, P., Bertozzi, C. R., Hart, G. W., and Etzler, M. E. (eds) (2009) *Essentials of Glycobiology*,

pp. 229–248, Cold Spring Harbor Laboratory Press, Cold Spring Harbor, NY
5. Heinegård, D. (2009) Proteoglycans and more from molecules to biology. *Int. J. Exp. Pathol.* **90,** 575–586
6. Chuang, C. Y., Lord, M. S., Melrose, J., Rees, M. D., Knox, S. M., Freeman, C., Iozzo, R. V., and Whitelock, J. M. (2010) Heparan sulfate-dependent signaling of fibroblast growth factor 18 by chondrocyte-derived perlecan. *Biochemistry* **49,** 5524–5532
7. Cortes, M., Baria, A. T., and Schwartz, N. B. (2009) Sulfation of chondroitin sulfate proteoglycans is necessary for proper Indian hedgehog signaling in the developing growth plate. *Development* **136,** 1697–1706
8. Gandhi, N. S., and Mancera, R. L. (2008) The structure of glycosaminoglycans and their interactions with proteins. *Chem. Biol. Drug Des.* **72,** 455–482
9. Mundlos, S., and Olsen, B. R. (1997) Heritable diseases of the skeleton. Part II: Molecular insights into skeletal development-matrix components and their homeostasis. *FASEB J.* **11,** 227–233
10. Schwartz, N. B., and Domowicz, M. (2002) Chondrodysplasias due to proteoglycan defects. *Glycobiology* **12,** 57R–68R
11. Bennett, E. P., Mandel, U., Clausen, H., Gerken, T. A., Fritz, T. A., and Tabak, L. A. (2012) Control of mucin-type *O*-glycosylation: a classification of the polypeptide GalNAc-transferase gene family. *Glycobiology* **22,** 736–756
12. Frishberg, Y., Ito, N., Rinat, C., Yamazaki, Y., Feinstein, S., Urakawa, I., Navon-Elkan, P., Becker-Cohen, R., Yamashita, T., Araya, K., Igarashi, T., Fujita, T., and Fukumoto, S. (2007) Hyperostosis-hyperphosphatemia syndrome: a congenital disorder of *O*-glycosylation associated with augmented processing of fibroblast growth factor 23. *J. Bone Miner. Res.* **22,** 235–242
13. Ichikawa, S., Guigonis, V., Imel, E. A., Courouble, M., Heissat, S., Henley, J. D., Sorenson, A. H., Petit, B., Lienhardt, A., and Econs, M. J. (2007) Novel GALNT3 mutations causing hyperostosis-hyperphosphatemia syndrome result in low intact fibroblast growth factor 23 concentrations. *J. Clin. Endocrinol. Metab.* **92,** 1943–1947
14. Ichikawa, S., Sorenson, A. H., Austin, A. M., Mackenzie, D. S., Fritz, T. A., Moh, A., Hui, S. L., and Econs, M. J. (2009) Ablation of the Galnt3 gene leads to low-circulating intact fibroblast growth factor 23 (Fgf23) concentrations and hyperphosphatemia despite increased Fgf23 expression. *Endocrinology* **150,** 2543–2550
15. Olauson, H., Krajisnik, T., Larsson, C., Lindberg, B., and Larsson, T. E. (2008) A novel missense mutation in GALNT3 causing hyperostosis-hyperphosphataemia syndrome. *Eur. J. Endocrinol.* **158,** 929–934
16. Topaz, O., Shurman, D. L., Bergman, R., Indelman, M., Ratajczak, P., Mizrachi, M., Khamaysi, Z., Behar, D., Petronius, D., Friedman, V., Zelikovic, I., Raimer, S., Metzker, A., Richard, G., and Sprecher, E. (2004) Mutations in GALNT3, encoding a protein involved in *O*-linked glycosylation, cause familial tumoral calcinosis. *Nat. Genet.* **36,** 579–581
17. Inada, M., Yasui, T., Nomura, S., Miyake, S., Deguchi, K., Himeno, M., Sato, M., Yamagiwa, H., Kimura, T., Yasui, N., Ochi, T., Endo, N., Kitamura, Y., Kishimoto, T., and Komori, T. (1999) Maturational disturbance of chondrocytes in Cbfa1-deficient mice. *Dev. Dyn.* **214,** 279–290
18. Kim, I. S., Otto, F., Zabel, B., and Mundlos, S. (1999) Regulation of chondrocyte differentiation by Cbfa1. *Mech. Dev.* **80,** 159–170
19. Enomoto, H., Furuichi, T., Zanma, A., Yamana, K., Yoshida, C., Sumitani, S., Yamamoto, H., Enomoto-Iwamoto, M., Iwamoto, M., and Komori, T. (2004) Runx2 deficiency in chondrocytes causes adipogenic changes *in vitro*. *J. Cell Sci.* **117,** 417–425
20. Enomoto, H., Shiojiri, S., Hoshi, K., Furuichi, T., Fukuyama, R., Yoshida, C. A., Kanatani, N., Nakamura, R., Mizuno, A., Zanma, A., Yano, K., Yasuda, H., Higashio, K., Takada, K., and Komori, T. (2003) Induction of osteoclast differentiation by Runx2 through receptor activator of nuclear factor-κB ligand (RANKL) and osteoprotegerin regulation and partial rescue of osteoclastogenesis in Runx2$^{-/-}$ mice by RANKL transgene. *J. Biol. Chem.* **278,** 23971–23977
21. Young, W. W., Jr., Holcomb, D. R., Ten Hagen, K. G., and Tabak, L. A. (2003) Expression of UDP-GalNAc:polypeptide *N*-acetylgalactosaminyltransferase isoforms in murine tissues determined by real-time PCR: a new view of a large family. *Glycobiology* **13,** 549–557
22. Miyazaki, T., Mori, M., Yoshida, C. A., Ito, C., Yamatoya, K., Moriishi, T., Kawai, Y., Komori, H., Kawane, T., Izumi, S. I., Toshimori, K., and Komori, T. (2013) Galnt3 deficiency disrupts acrosome formation and leads to oligoasthenoteratozoospermia. *Histochem. Cell Biol.* **139,** 339–354
23. Krebsbach, P. H., Nakata, K., Bernier, S. M., Hatano, O., Miyashita, T., Rhodes, C. S., and Yamada, Y. (1996) Identification of a minimum enhancer sequence for the type II collagen gene reveals several core sequence motifs in common with the link protein gene. *J. Biol. Chem.* **271,** 4298–4303
24. Ueta, C., Iwamoto, M., Kanatani, N., Yoshida, C., Liu, Y., Enomoto-Iwamoto, M., Ohmori, T., Enomoto, H., Nakata, K., Takada, K., Kurisu, K., and Komori, T. (2001) Skeletal malformations caused by overexpression of Cbfa1 or its dominant negative form in chondrocytes. *J. Cell Biol.* **153,** 87–100
25. Zhou, G., Garofalo, S., Mukhopadhyay, K., Lefebvre, V., Smith, C. N., Eberspaecher, H., and de Crombrugghe, B. (1995) A 182 bp fragment of the mouse pro α 1(II) collagen gene is sufficient to direct chondrocyte expression in transgenic mice. *J. Cell Sci.* **108,** 3677–3684
26. Komori, T., Yagi, H., Nomura, S., Yamaguchi, A., Sasaki, K., Deguchi, K., Shimizu, Y., Bronson, R. T., Gao, Y. H., Inada, M., Sato, M., Okamoto, R., Kitamura, Y., Yoshiki, S., and Kishimoto, T. (1997) Targeted disruption of Cbfa1 results in a complete lack of bone formation owing to maturational arrest of osteoblasts. *Cell* **89,** 755–764
27. Kato, K., Takeuchi, H., Ohki, T., Waki, M., Usami, K., Hassan, H., Clausen, H., and Irimura, T. (2008) A lectin recognizes differential arrangements of *O*-glycans on mucin repeats. *Biochem. Biophys. Res. Commun.* **371,** 698–701
28. Wu, A. M., Sugii, S. J., and Herp, A. (1988) A guide for carbohydrate specificities of lectins. *Adv. Exp. Med. Biol.* **228,** 819–847
29. Kiviranta, I., Tammi, M., Jurvelin, J., Säämänen, A. M., and Helminen, H. J. (1985) Demonstration of chondroitin sulphate and glycoproteins in articular cartilage matrix using periodic acid-Schiff (PAS) method. *Histochemistry* **83,** 303–306
30. Gerlitz, B., Hassell, T., Vlahos, C. J., Parkinson, J. F., Bang, N. U., and Grinnell, B. W. (1993) Identification of the predominant glycosaminoglycan-attachment site in soluble recombinant human thrombomodulin: potential regulation of functionality by glycosyltransferase competition for serine 474. *Biochem. J.* **295,** 131–140
31. Chen, L., Wu, Y., Lee, V., Kiani, C., Adams, M. E., Yao, Y., and Yang, B. B. (2002) The folded modules of aggrecan G3 domain exert two separable functions in glycosaminoglycan modification and product secretion. *J. Biol. Chem.* **277,** 2657–2665
32. Kiani, C., Lee, V., Cao, L., Chen, L., Wu, Y., Zhang, Y., Adams, M. E., and Yang, B. B. (2001) Roles of aggrecan domains in biosynthesis, modification by glycosaminoglycans and product secretion. *Biochem. J.* **354,** 199–207
33. Alonso, M., Hidalgo, J., Hendricks, L., and Velasco, A. (1996) Degradation of aggrecan precursors within a specialized subcompartment of the chicken chondrocyte endoplasmic reticulum. *Biochem. J.* **316,** 487–495
34. Sato, T., Kudo, T., Ikehara, Y., Ogawa, H., Hirano, T., Kiyohara, K., Hagiwara, K., Togayachi, A., Ema, M., Takahashi, S., Kimata, K., Watanabe, H., and Narimatsu, H. (2011) Chondroitin sulfate *N*-acetylgalactosaminyltransferase 1 is necessary for normal endochondral ossification and aggrecan metabolism. *J. Biol. Chem.* **286,** 5803–5812
35. Fukuda, M. (2002) Roles of mucin-type *O*-glycans in cell adhesion. *Biochim. Biophys. Acta* **1573,** 394–405
36. Carraway, K. L., Ramsauer, V. P., Haq, B., and Carothers Carraway, C. A. (2003) Cell signaling through membrane mucins. *BioEssays* **25,** 66–71
37. Singh, P. K., and Hollingsworth, M. A. (2006) Cell surface-associated mucins in signal transduction. *Trends Cell Biol.* **16,** 467–476
38. Breuza, L., Garcia, M., Delgrossi, M. H., and Le Bivic, A. (2002) Role of the membrane-proximal *O*-glycosylation site in sorting of the human receptor for neurotrophins to the apical membrane of MDCK cells. *Exp. Cell Res.* **273,** 178–186
39. Zheng, X., and Sadler, J. E. (2002) Mucin-like domain of enteropeptidase directs apical targeting in Madin-Darby canine kidney cells. *J. Biol. Chem.* **277,** 6858–6863
40. Patsos, G., Robbe-Masselot, C., Klein, A., Hebbe-Viton, V., Martin, R. S., Masselot, D., Graessmann, M., Paraskeva, C., Gallagher, T., and Corfield,

A. (2007) *O*-Glycan regulation of apoptosis and proliferation in colorectal cancer cell lines. *Biochem. Soc. Trans.* **35,** 1372–1374
41. Taniuchi, K., Cerny, R. L., Tanouchi, A., Kohno, K., Kotani, N., Honke, K., Saibara, T., and Hollingsworth, M. A. (2011) Overexpression of GalNAc-transferase GalNAc-T3 promotes pancreatic cancer cell growth. *Oncogene* **30,** 4843–4854
42. Wu, Y. M., Liu, C. H., Hu, R. H., Huang, M. J., Lee, J. J., Chen, C. H., Huang, J., Lai, H. S., Lee, P. H., Hsu, W. M., Huang, H. C., and Huang, M. C. (2011) Mucin glycosylating enzyme GALNT2 regulates the malignant character of hepatocellular carcinoma by modifying the EGF receptor. *Cancer Res.* **71,** 7270–7279
43. Garner, B., Merry, A. H., Royle, L., Harvey, D. J., Rudd, P. M., and Thillet, J. (2001) Structural elucidation of the *N*- and *O*-glycans of human apolipoprotein(a): role of *O*-glycans in conferring protease resistance. *J. Biol. Chem.* **276,** 22200–22208
44. Kato, K., Jeanneau, C., Tarp, M. A., Benet-Pagès, A., Lorenz-Depiereux, B., Bennett, E. P., Mandel, U., Strom, T. M., and Clausen, H. (2006) Polypeptide GalNAc-transferase T3 and familial tumoral calcinosis. Secretion of fibroblast growth factor 23 requires *O*-glycosylation. *J. Biol. Chem.* **281,** 18370–18377
45. Schjoldager, K. T., and Clausen, H. (2012) Site-specific protein *O*-glycosylation modulates proprotein processing: deciphering specific functions of the large polypeptide GalNAc-transferase gene family. *Biochim. Biophys. Acta* **1820,** 2079–2094
46. St-Jacques, B., Hammerschmidt, M., and McMahon, A. P. (1999) Indian hedgehog signaling regulates proliferation and differentiation of chondrocytes and is essential for bone formation. *Genes Dev.* **13,** 2072–2086
47. Vortkamp, A., Lee, K., Lanske, B., Segre, G. V., Kronenberg, H. M., and Tabin, C. J. (1996) Regulation of rate of cartilage differentiation by Indian hedgehog and PTH-related protein. *Science* **273,** 613–622
48. Shu, B., Zhang, M., Xie, R., Wang, M., Jin, H., Hou, W., Tang, D., Harris, S. E., Mishina, Y., O'Keefe, R. J., Hilton, M. J., Wang, Y., and Chen, D. (2011) BMP2, but not BMP4, is crucial for chondrocyte proliferation and maturation during endochondral bone development. *J. Cell Sci.* **124,** 3428–3440
49. Lohmander, L. S., De Luca, S., Nilsson, B., Hascall, V. C., Caputo, C. B., Kimura, J. H., and Heinegard, D. (1980) Oligosaccharides on proteoglycans from the swarm rat chondrosarcoma. *J. Biol. Chem.* **255,** 6084–6091

Overexpression of *Galnt3* in Chondrocytes Resulted in Dwarfism Due to the Increase of Mucin-type *O*-Glycans and Reduction of Glycosaminoglycans

Carolina Andrea Yoshida, Tetsuya Kawane, Takeshi Moriishi, Anurag Purushothaman, Toshihiro Miyazaki, Hisato Komori, Masako Mori, Xin Qin, Ayako Hashimoto, Kazuyuki Sugahara, Kei Yamana, Kenji Takada and Toshihisa Komori

J. Biol. Chem. 2014, 289:26584-26596.
doi: 10.1074/jbc.M114.555987 originally published online August 8, 2014
